THE KONDO-LATTICE MODEL AND THE KONDO-SPIN GLASS COMPETITION IN HEAVY FERMION SYSTEMS*

B. Coqblin
Laboratoire de Physique des Solides, Université Paris-Sud, 91405-Orsay, France
M. A. Gusmão, J. R. Iglesias, Alba Theumann
Instituto de Física, U.F.R.G.S., C.P. 15051, 91501-970 Porto Alegre, RS, Brazil
C. Lacroix
Laboratoire L. Néel, CNRS, BP 166, 38042-Grenoble Cedex 09, France
S. G. Magalhães
Departamento de Física, U.F.S.M., 97105-900 Santa Maria, RS, Brazil
and A.A. Schmidt
Departamento de Matemática, U.F.S.M., 97105-900 Santa Maria, RS, Brazil

(Received July 10, 2002)

Many cerium or ytterbium alloys and compounds are characterized by heavy-fermion behavior due to the Kondo effect. In the case of a lattice, there is a strong competition between the Kondo effect and magnetic ordering. The magnetic order close to the quantum critical point(QCP) is generally an antiferromagnetic one, but could be also a ferromagnetic one or a spin-glass one in disordered systems. We review here the main features of the Kondo lattice model within a mean-field treatment of the Hamiltonian, including both the s–f exchange intra-site interaction and the nearest neighbor inter-site f–f interaction. First, we study the non-magnetic case and discuss the effects of conduction band filling and of the inter-site exchange parameter on the occurrence of the Kondo effect and short-range magnetic correlations. Second, we treat the spin glass-Kondo competition by considering a random inter-site interaction and we study the competition between Kondo, spin-glass and ferromagnetic phases. The nature of the transition at the QCP is also discussed and comparison with experimental data in heavy fermions systems is finally presented.

PACS numbers: 71.27.+a, 75.30.Mb, 75.20.Hr, 75.10.Nr

* Presented at the International Conference on Strongly Correlated Electron Systems, (SCES 02), Cracow, Poland, July 10–13, 2002.

1. Introduction

The properties of many cerium or ytterbium compounds are well understood in the theoretical framework of the Kondo effect. The single-impurity Kondo effect has been exactly solved [1]: at low temperatures, the system has a "Fermi Liquid" behavior with a T^2 behavior of the electrical resistivity and very large values of both the electronic constant of the specific heat and the magnetic susceptibility, which were at the origin of the name "heavy fermions" given to these systems [2–4]. At high temperatures with respect to the Kondo temperature, the magnetic contribution to the electrical resistivity is generally passing through a maximum corresponding to the overall crystal field splitting and decreasing then as Log T [5]. More recently, some cerium or uranium compounds have been observed to become superconducting at low temperatures, either at normal pressure or under high pressures [6–8].

On the other hand, in the case of a lattice, there exists a strong competition between the Kondo effect and magnetic ordering, arising from the RKKY (Ruderman–Kittel–Kasuya–Yosida) interaction between rare-earth atoms at different lattice sites. This situation is well described by the Doniach diagram, [9] which gives the variation of the Néel temperature and of the Kondo temperature with increasing antiferromagnetic intrasite exchange interaction J_{K} between localized spins and conduction-electron spins. If one considers the exchange Hamiltonian between localized ($\boldsymbol{S}$) and conduction-electron ($\boldsymbol{s}$) spins, given by

$$H = J_{\mathrm{K}}\, \boldsymbol{s} \cdot \boldsymbol{S} \tag{1}$$

usual theories of the one-impurity Kondo effect and of the RKKY interaction yield a Kondo temperature T_{K0}, that is proportional to $\exp(-1/\rho J_{\mathrm{K}})$, and an ordering temperature (Néel or, in some cases, Curie), T_{N0}, proportional to ρJ_{K}^2, ρ being the density of states for the conduction band at the Fermi energy. Thus, for small ρJ_{K} values, T_{N0} is larger than T_{K0} and the system tends to order magnetically, with often a reduction of the magnetic moment due to the Kondo effect; on the contrary, for large ρJ_{K}, T_{K0} is larger than T_{N0} and the system tends to become non magnetic. The actual ordering temperature T_{N}, therefore, increases initially with increasing ρJ_{K}, then passes through a maximum and tends to zero at a critical value $\rho J_{\mathrm{K}}^{\mathrm{c}}$ corresponding to a "quantum critical point" (QCP) in the Doniach diagram. Such a behavior of T_{N} has been experimentally observed with increasing pressure in many Kondo compounds, such as for example in $CeAl_2$ (Ref. [10]) or in $CeRh_2Si_2$ [11]. Thus, we can conclude that the variation of the Néel temperature predicted by the Doniach diagram is well observed experimentally in many cerium compounds. We also know that the Néel temperature

starts from zero at a given pressure, and increases rapidly with pressure in $YbCu_2Si_2$ (Ref. [12]) or in related ytterbium compounds, which can be considered as another check of the Doniach diagram.

The one-impurity model predicts an exponential increase of the Kondo temperature with ρJ_K. This means that the Kondo temperature should increase with increasing pressure in cerium compounds and with decreasing pressure in ytterbium compounds, which agrees well with many observations. However, deviations seem to occur in some cerium compounds, such as $CeRh_2Si_2$ (Ref. [11]) or $CeRu_2Ge_2$, [13,14] where the actual Kondo temperature observed in a lattice can be significantly different from the one derived for the single-impurity case. Thus, in order to account for such an effect, we have studied in detail the Kondo-lattice model within a mean-field approximation and with both intrasite Kondo exchange and intersite antiferromagnetic exchange, treating successively the half-filled case (corresponding to a number of conduction electrons $n = 1$) [16] and then the general case $n < 1$ [17–20] which gives a much better description of the metallic cerium systems. This approach has been performed in the non-magnetic regime and we will describe in the next section the main results and particularly the most recent ones [20].

The second extensively studied question concerns the transition from a magnetically ordered regime (which could be antiferromagnetic, ferromagnetic, spin glass ...) to the non magnetic heavy fermion regime observed in the Doniach diagram. The transition from an antiferromagnetic regime to a Kondo one had been studied theoretically and gives a qualitative agreement with the Doniach diagram [21]; but the obtained transition is a first-order one without QCP. We will not discuss here this case which has been already described in Ref. [21].

On the other hand, a spin glass state or an heterogenous disordered alloy with magnetic clusters has been observed in several disordered cerium alloys such as for example the Ce(Ni,Cu) alloys [22,23]. We have studied the Spin Glass-Kondo transition within the same approximation [24] and we will discuss in the third section the different features of this transition, including the possibility of a ferromagnetic-Spin Glass-Kondo phase sequence [25] and the existence of a Quantum Critical Point in the phase diagram.

2. Band filling effects in the Kondo-lattice

We have seen in the introduction that the Doniach diagram describes well the behavior of the Neel temperature T_N *versus* ρJ_K or increasing pressure in cerium compounds and decreasing pressure in ytterbium compounds. On the other hand, the one-impurity model predicts an exponential increase of the Kondo temperature with ρJ_K, which agrees with the observed variation

of T_K in many cerium or ytterbium systems. However, deviations seem to occur in some cerium compounds, such as $CeRh_2Si_2$, [11] $CeRu_2Ge_2$, [13,14] or more recently [15] $Ce_2Rh_3Ge_5$, where the actual Kondo temperature observed in a lattice can be significantly different from the single-impurity one. Moreover, short-range magnetic correlations between neighboring cerium atoms have been observed by neutron diffraction experiments in single crystals of $CeCu_6$, [26] $CeInCu_2$, [27] $CeRu_2Si_2$, [26,28,29] or $Ce_{1-x}La_xRu_2Si_2$ (Refs. [28–31]) at low temperatures. The experimentally observed "correlation temperature" T_{cor}, below which short-range magnetic correlations between neighboring cerium atoms occur, is clearly larger than the Kondo temperature T_K : $T_{cor} \sim$ 60–70 K and $T_K \sim$ 20 K in $CeRu_2Si_2$; [26,28,29] $T_{cor} \sim$ 10 K and $T_K \sim$ 5 K in $CeCu_6$, [26].

In order to account for these experimental results, we have introduced a Kondo-lattice model with both an intrasite Kondo exchange interaction and an intersite antiferromagnetic exchange interaction in the half-filled case [16]. We employed a mean-field approximation and we have shown that the enhancement of the intersite exchange interaction tends to decrease the Kondo temperature T_K for the lattice with respect to the one-impurity Kondo temperature T_{K0} [16]. However, when $n < 1$, an "exhaustion" problem arises, which means that there are not enough conduction electrons to screen all the localized spins and, as a consequence, the Kondo temperature decreases [32,33].

The Kondo-lattice model has been firstly studied with only the intrasite Kondo interaction [34–36]. In particular, Continentino *et al.*, [35] using scaling theory, have found a coherence temperature increasing above the QCP. More recently, Nozières, [33] and Burdin *et al.*, [37,38] have studied the exhaustion limit and have obtained a zero-temperature energy gain, T^*, related to the coherent Kondo effect. The effect of a small number of conduction electrons has been also studied within both the Kondo-lattice and the Anderson-lattice models [39–42].

The proposed Hamiltonian of the system is, therefore,

$$H = \sum_{\boldsymbol{k}\sigma} \varepsilon_{\boldsymbol{k}} n^{c}_{\boldsymbol{k}\sigma} + J_K \sum_i \boldsymbol{s}_i \cdot \boldsymbol{S}_i + J_H \sum_{\langle ij \rangle} \boldsymbol{S}_i \cdot \boldsymbol{S}_j \,, \tag{2}$$

where $\varepsilon_{\boldsymbol{k}}$ is the energy of the conduction band, J_K is the Kondo coupling between a localized spin $\boldsymbol{S}_i$ and the spin $\boldsymbol{s}_i$ of a conduction electron at the same site, and J_H is the interaction between nearest-neighboring localized spins. Assuming spin-1/2 localized moments, we represented them by a zero-width f band with one electron per site, while the conduction band has width $2D$ and a constant density of states. We choose J_K and J_H to be positive, implying that both local and intersite interactions are antiferromagnetic.

We now write the spin operators in fermionic representation, remembering that we have a constraint of single-occupancy of the f level at all sites, $n_i^f = 1$. In order to discuss the Kondo effect and magnetic correlations we define the correlators

$$\lambda_{i\sigma} = c_{i\sigma}^{\dagger} f_{i\sigma}\,, \quad \Gamma_{ij\sigma} = f_{i\sigma}^{\dagger} f_{j\sigma}\,, \tag{3}$$

where $\lambda_{i\sigma}$ describes the intrasite Kondo correlation, and $\Gamma_{ij\sigma}$ represents an intersite correlation between two neighboring atoms. With this notation we perform an extended mean-field approximation, introduced by Coleman and Andrei, [43] and presented in full detail in Ref. [16]. Considering translational invariance, and taking into account that there is no breakdown of spin symmetry, *i.e.*, no magnetic states, we can write $\lambda_{i\sigma} = \langle \lambda_{i\sigma} \rangle$ for all sites, and $\Gamma = \langle \Gamma_{ij\sigma} \rangle$ for nearest-neighboring sites and zero otherwise. In this way we obtain a mean-field Hamiltonian that takes the form of a hybridized two-band system:

$$\begin{aligned} H^{\mathrm{MF}} \;=\; & \sum_{\boldsymbol{k}\sigma} \varepsilon_{\boldsymbol{k}} n_{\boldsymbol{k}\sigma}^{\mathrm{c}} + E_0 \sum_i \left(\sum_\sigma n_{i\sigma}^f - 1 \right) \\ & - J_{\mathrm{K}} \lambda \sum_{i\sigma} \left(c_{i\sigma}^{\dagger} f_{i\sigma} + f_{i\sigma}^{\dagger} c_{i\sigma} \right) + \bar{E}_{\mathrm{K}} \\ & - J_{\mathrm{H}} \Gamma \sum_{\langle ij \rangle \sigma} \left(f_{i\sigma}^{\dagger} f_{j\sigma} + f_{j\sigma}^{\dagger} f_{i\sigma} \right) + \bar{E}_{\mathrm{H}}\,, \end{aligned} \tag{4}$$

with

$$\bar{E}_{\mathrm{K}} = 2N J_{\mathrm{K}} \lambda^2\,, \quad \bar{E}_{\mathrm{H}} = z N J_{\mathrm{H}} \Gamma^2\,, \tag{5}$$

N being the total number of lattice sites.

After performing this approximation, one deals with a one-electron Hamiltonian representing two hybridized bands: the conduction band of width $2D$ and the f band of effective band width $2BD$, with B given by

$$B = -z J_{\mathrm{H}} \Gamma / D, \tag{6}$$

z being the number of nearest neighbors of a site, while the magnitude of the hybridization gap is directly related to λ^2. This quantity is also a measure of the Kondo effect, as the Kondo correlation function $\langle \boldsymbol{s}_i \cdot \boldsymbol{S}_i \rangle$ is proportional to λ^2.

Leaving aside the constant terms, the Hamiltonian (4) is easily diagonalized, and the resulting energies of the two new hybrid bands are

$$\begin{aligned} E_{\boldsymbol{k}}^{\pm} \;=\; & \frac{1}{2} \Bigg[\varepsilon_{\boldsymbol{k}} (1 + B) + E_0 \\ & \pm \sqrt{\left[\varepsilon_{\boldsymbol{k}} (1 - B) - E_0 \right]^2 + 4 J_{\mathrm{K}}^2 \lambda^2} \Bigg]\,. \end{aligned} \tag{7}$$

The mean-field parameters λ and Γ are obtained by self-consistently solving Eqs. (3) or, equivalently, by minimizing the total internal energy at zero temperature, or the total free energy F at finite temperatures [17]. As usual, [16] the reference energy E_0 of the f band and the chemical potential μ have to be determined self-consistently in order to keep the average numbers of f and conduction electrons respectively equal to 1 and n.

We will now present the main results obtained for the general case $n < 1$. Preliminary results had been previously [19] presented and a full paper will be published soon [20] and detailed calculations at both $T = 0$ and finite temperatures can be found there.

The two hybridized bands $E^{\pm}_{\boldsymbol{k}}$ given by Eq. (7) exhibit a structure that depends on the two factors $A \equiv J_{\mathrm{K}}^2 \lambda^2$ and B, defined by (6), and especially on the sign of B. In the case of $n = 1$, previously considered, [16] for small B values such that $|B|D^2 < A$ there is a gap, the lower band is completely full and the upper band empty at $T = 0$. For $n < 1$, the Fermi level cuts the lower band, and the upper band is still empty at $T = 0$, which corresponds, therefore, to a real metallic situation.

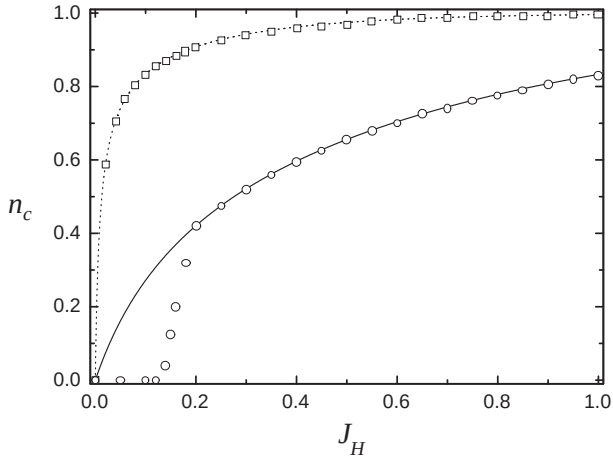

Fig. 1. Phase diagram plotted as the critical band filling n_{c} *versus* J_{H}. The curves are drawn from Eq. (8) for $J_{\mathrm{K}}/D = 0.4$ (dotted line) and 1.0 (solid line). The symbols correspond to the results obtained by minimizing the energy. In each case, the Kondo regime is stable above the line, and the magnetic phase below.

The shape of the lower band $E^{-}_{\boldsymbol{k}}$ and the solution of the case $n < 1$ depend critically and self-consistently on the values of the different parameters J_{K}, J_{H} and n. Thus, the shape of $E^{-}_{\boldsymbol{k}}$ can change under a variation of the parameters, and this peculiar situation makes the problem difficult to solve [20]. We present here just the phase diagram obtained at $T = 0$ for $J_{\mathrm{K}}/D = 0.4$ and 1.0 (figure 1), where the Kondo phase is characterized

by $\lambda \neq 0$. In the latter case, for small $J_{\rm H}$, the Kondo phase is stable for all values of the band filling, while for large $J_{\rm H}$ the Kondo phase is stable only for $n > n_{\rm c}$ given by [20]:

$$n_{\rm c} = 1 - (1 - B)\sqrt{\frac{u}{u - B}}\,, \tag{8}$$

with:

$$u \;=\; \exp\left[-2D(1 - B)/J_{\rm K}\right]\,. \tag{9}$$

Figure 1 also shows that Eq. (8) is very close to the numerical result in this region. The crossover between the two regimes was obtained numerically. In the crossover region we found a *discontinuous* transition from $\lambda \neq 0$ to $\lambda = 0$. These results have to be taken with caution, however, since the value of $J_{\rm K}/D = 1$ is unphysically high, and also the Kondo lattice is expected to show ferromagnetic behavior in the low-n limit, [36] while our analysis is restricted to antiferromagnetic intersite exchange.

Thus, our calculation shows clearly that small n and large $J_{\rm H}$ values tend to suppress the Kondo effect, yielding a "magnetic" phase with $\lambda = 0$ and large short-range magnetic correlations. In fact, in this region a long-range magnetic order should certainly be stabilized, but this was not taken into account in this approach. In contrast, both λ and Γ are different from zero in the Kondo phase.

Then, we look at the Kondo-lattice problem at finite temperatures, for the general case of $n < 1$. The values of λ and Γ are determined by self-consistently solving Eqs. (3) or by minimizing the free energy [20]. In our mean-field approximation, $T_{\rm K}$ and $T_{\rm cor}$ are defined as the temperatures at which respectively λ and Γ become zero. Results obtained at finite temperatures in the case $n < 1$, for different sets of parameters $J_{\rm K}$, $J_{\rm H}$ and n are presented in detail elsewhere [20] and we will summarize them here. Figure 2 gives the curves of the Kondo temperature $T_{\rm K}$ *versus* $J_{\rm H}$ for a given $J_{\rm K}$ value and several values of the conduction band-filling n. We see clearly that $T_{\rm K}$ first increases, and then decreases with $J_{\rm H}$ for fixed n, dropping abruptly to zero at some critical value of $J_{\rm H}$. On the other hand, for a given $J_{\rm H}$, $T_{\rm K}$ decreases rapidly as n departs from half filling. We have also plotted $T_{\rm cor}$ which is linear with $J_{\rm H}$, independently of the considered value of n [16]. Figure 3 gives $T_{\rm K}$ as a function of $J_{\rm K}$ for $J_{\rm H}/D = 0.04$ and representative values of n. Here again we include the correlation temperature $T_{\rm cor}$, which signals the onset of short-range magnetic correlations when the temperature is lowered at fixed $J_{\rm K}$. For comparison, we plot the single-impurity Kondo temperature $T_{\rm K0}$, which varies exponentially with $J_{\rm K}$, and is weakly dependent on n near half-filling.

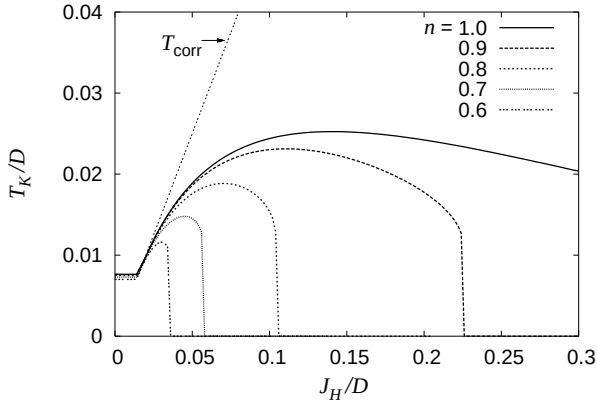

Fig. 2. Plot of the Kondo temperature T_{K} *versus* J_{H} for $J_{\mathrm{K}}/D = 0.4$ and several values of n. We also show the correlation temperature T_{cor}.

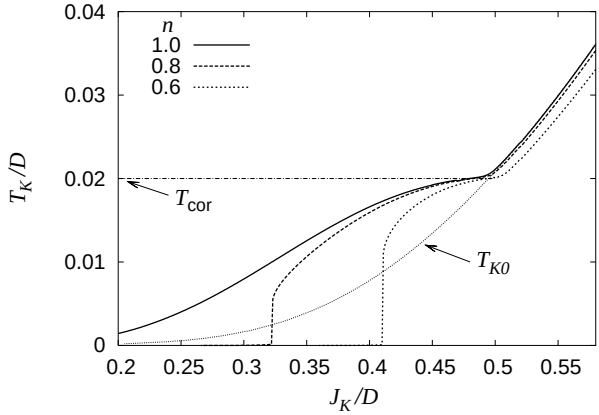

Fig. 3. Plot of the Kondo temperature T_{K} as a function of J_{K} for $J_{\mathrm{H}}/D = 0.04$ and representative values of n. We also show the correlation temperature T_{cor}, and the single-impurity Kondo temperature T_{K0}.

Figures 2 and 3 show some interesting results of our model. First, one can see the occurrence of short-range magnetic correlations above the Kondo temperature, in good agreement with experiment. Also, in the region of coexistence between Kondo effect and magnetic correlations, the Kondo temperature, although enhanced with respect to the single-impurity case, shows a smoother variation with J_{K}. The second noticeable feature of Figs. 2 and 3 is the almost catastrophic suppression of the Kondo effect with increasing intersite coupling, and the enhancement of this behavior as the band-filling factor is reduced. However, we remark that a small value of the intersite interaction J_{H} reinforces the Kondo effect by increasing the Kondo temperature.

So, we have established here for $n < 1$, as in the previous work [16] for $n = 1$, that the dependence of the Kondo temperature with the coupling constant J_K for the lattice can be significantly different from the single-impurity case. This result can account for the pressure dependence of T_K observed in $CeRh_2Si_2$, [11] $CeRu_2Ge_2$, [13,14] and $Ce_2Rh_3Ge_5$ [15]. On the other hand, depending on the relative values of J_H and J_K, as well as on the band-filling, the lattice Kondo temperature can also follow the single-impurity one, as observed in many cerium and all ytterbium compounds. Further experiments are needed to better understand the conditions yielding a Kondo temperature for the lattice much different than the single-impurity one. This issue has also been addressed by different theoretical approaches to both the Kondo lattice and the Periodic Anderson Model [35,37,39–41,44].

Another interesting result concerns the derivation of a correlation temperature below which short-range magnetic correlations appear, in good agreement with neutron scattering experiments in cerium compounds. These correlations can coexist with the Kondo effect and eventually dominate, and suppress the Kondo regime for sufficiently high values of the intersite exchange interaction or sufficiently low band fillings.

Our present calculation addresses again the difficult issue of the nature of the ground state and screening in the Kondo-lattice problem. We have shown here that, as the number of conduction electrons is reduced, exhaustion may be compensated by formation of intersite singlets of localized spins. Finally, it is interesting to notice that taking into account lattice effects can be important for describing the properties of cerium or other anomalous rare-earth compounds at low temperatures, as shown, for example, in photoemission experiments [41,42,45].

3. The competition between spin glass and Kondo effect

The second subject we would like to describe here concerns the competition between the Kondo effect and a spin glass order. It is well known that there is a strong competition between the Kondo effect and a magnetic order (mostly antiferromagnetic and in some cases ferromagnetic) shown in the Doniach diagram, as presented in the introduction. It is also established that, in the vicinity of the QCP, several different "Non Fermi Liquid" (NFL) behaviors have been observed in addition to the well-known "Fermi Liquid" behavior.

But, in the case of disordered cerium alloys, the disorder can yield a Spin Glass (SG) phase in addition to the NFL behavior at low temperatures around the QCP. The magnetic phase diagram of $CeNi_{1-x}Cu_x$ has been extensively studied [22,23]. CeCu is antiferromagnetic below 3.5 K and CeNi is a non magnetic compound with an intermediate valence. The low temper-

ature antiferromagnetic phase changes, around $x = 0.8$, to a ferromagnetic one which finally disappears around $x = 0.2$. At higher temperatures, a Spin Glass state is deduced from all measured bulk properties, such as the AC susceptibility; for example, for $x = 0.6$, the SG state exists between 2 K and the ferromagnetic Curie temperature $T_c = 1.1K$. At $x = 0.2$, the SG phase exists below 6 K and for $x < 0.2$ a Kondo behavior has been proposed; finally CeNi is an intermediate valence compound. Thus, in the $CeNi_{1-x}Cu_x$ system at very low temperatures, for $x < 0.7$, the phase sequence FM-SG-Kondo has been observed with decreasing x and in the range 0.7–0.2, the sequence FM-SG is obtained with increasing temperature.

An unusual interplay between Kondo effect and spin-glass behavior has been recently observed in several other disordered cerium systems such as $CeCoGe_{3-x}Si_x$, [46], $Ce_2Au_{1-x}Co_xSi_3$, [47] or $Ce_2Pd_{1-x}Co_xSi_3$ alloys [48]. In particular, an antiferromagnetic phase exists at low temperatures between the spin glass phase and the Kondo one just below the QCP and the sequence of SG-AF-Kondo phases is, therefore, obtained with increasing x in $Ce_2Au_{1-x}Co_xSi_3$ alloys [47]. NFL and spin glass behaviors have been also observed in disordered uranium alloys [49], as for example a sequence of AF-NFL-SG phases in $UCu_{5-x}Pd_x$ alloys [50] or the opposite sequence AF-SG-NFL in $U_{1-x}La_xPd_2Al_3$ alloys [51].

We would like to present here some recent theoretical works that describe the competition between the spin glass and the Kondo phases [24] and more recently the SG-Kondo-Ferromagnetic phase transitions [25]. The model is based on the previously described Kondo lattice model with an intrasite s–f exchange interaction and an intersite long range random interaction that couples the localized spins, like in the Sherrington–Kirkpatrick spin glass model [52]. The use of the static approximation and the replica symmetry ansatz has made possible to solve the problem at a mean field level. This fermionic problem is formulated by representing the spin operators as bilinear combinations of Grassmann fields and the partition function is found through the functional integral formalism [53]. We describe here two cases, by taking the mean random interaction J_0 firstly equal to zero in order to describe the SG-Kondo transition and then different from zero in order to produce a ferromagnetic ordering and to describe the SG-Kondo-Ferromagnetic phase sequence.

To describe the Kondo effect in a mean-field-like theory it is sufficient to keep only the spin-flip terms in the exchange Hamiltonian, while the spin glass interaction is represented by a quantum Ising Hamiltonian where the only interaction is between the z-components of the localized spins [25, 53, 54].

So, the model used here to study a spin glass ordering in a Kondo lattice compound is described by the general Hamiltonian

$$\mathcal{H} - \mu_{\rm c} N_{\rm c} - \mu_f N_f \;=\; \mathcal{H}_0 = \sum_{k,\sigma} \epsilon_k n_{k\sigma} + \epsilon_0 \sum_{i,\sigma} n_{i\sigma}^f + J_{\rm K} \sum_i [S_{fi}^+ s_i^- + S_{fi}^- s_i^+] - \sum_{i,j} J_{ij} S_{fi}^z S_{fj}^z \,, \quad (10)$$

where $J_{\rm K} > 0$ and the sum runs over N lattice sites. In the present case the random intersite interaction J_{ij} in the Hamiltonian is an independent random variable with a gaussian distribution

$$P(J_{ij}) = e^{-(J_{ij} - < J_{ij} >)^2 \frac{N}{16 J^2}} \sqrt{\frac{N}{16 \pi J^2}} \,. \quad (11)$$

In the first paper [24], we have taken an average $< J_{ij} >= 0$ and more recently in order to describe the sequence of SG-Kondo-Ferromagnetic phases [25], we have taken a non-zero value $\langle J_{ij} \rangle = 2J_0/N$.

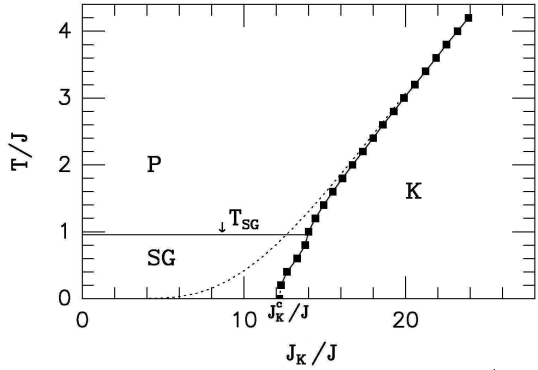

Fig. 4. Phase diagram in the T–$J_{\rm K}$ plane as a function of T/J and $J_{\rm K}/J$ for fixed $J = 0.05D$, where D is the conduction bandwidth. The dotted line represents the "pure" Kondo temperature $T_{\rm K}$.

Numerical solutions for the first studied case [24] are presented in Fig. 4 which gives a magnetic phase diagram in the $J_{\rm K}$ *vs.* T plane. At high temperatures, the "normal" phase is paramagnetic with vanishing Kondo and spin glass order parameters, *i.e.* $\lambda = q = 0$. When temperature is lowered, for not too large values of the ratio $J_{\rm K}/J$, a second-order transition line is found at $T = T_{\rm SG}$ to a spin glass phase with $q > 0$ and $\lambda = 0$. Finally, for large values of the ratio $J_{\rm K}/J$, we recover the "Kondo" phase with a non-zero λ value and $q = 0$: the transition line from the paramagnetic phase to the Kondo phase for temperatures larger than $T_{\rm SG}$ is a second-order one and

occurs at a temperature very close to the one-impurity Kondo temperature T_{K0}. On the other hand, the transition line from the spin-glass phase to the Kondo phase, for temperatures smaller than T_{SG}, is a first-order one and ends at J_K^c at $T = 0$; the separation between the spin-glass and the Kondo phases departs there completely from the behavior of T_{K0}. We can also remark that we get here only "pure" Kondo or SG phases and never a mixed SG-Kondo phase with the two order parameters different from zero; this result is probably connected to the approximations used here to treat the starting Hamiltonian.

The diagram shown in figure 4 can account partly for the magnetic phase diagram observed above the Curie temperature for the $CeNi_{1-x}Cu_x$ alloys [23] for small x values when there is a transition from a spin-glass state to a Kondo state. However, the experimental phase diagrams are generally more complicated and present an antiferromagnetic or a ferromagnetic phase in addition to the Kondo and SG phases. Thus, we have extended the previous model, in order to include the proper elements that produce also a ferromagnetic ordering by taking the mean random interaction J_0 different from zero. Therefore, the magnetization m can be introduced as a new order parameter, in addition to the two other order parameters and solved coupled to them. As previously done, the static approximation and replica symmetry ansatz lead to a mean field solution of the problem. The resulting coupled saddle point equations for the order parameters produce solutions which give a Kondo state, a magnetic ordering like ferromagnetism, a spin glass phase and a mixed (ferromagnetic-spin glass) one.

Detailed calculations and results can be found in the full paper [25] and we will present here briefly the results concerning the occurrence of the ferromagnetic phase in addition to the spin glass and Kondo phases which have been described in Ref. [24]. Fig. 5 shows the evolution of the phase diagram with increasing values of J_0/J. For small values of J_0/J, the phase diagram shown in figure 5(a) is essentially the same as that shown in Fig. 4 for $J_0 = 0$ [24], with a paramagnetic, a spin glass and a Kondo phase. When the value of J_0 increases above a critical value, the phase diagram starts to show the presence of a ferromagnetic phase which has a transition temperature $T_c(J_0)$ increasing with J_0. Thus, in the two cases shown in figures 5(b) and (c), for decreasing temperature, first a transition from a paramagnetic to a ferromagnetic phase appears followed by a transition from the ferromagnetic to a "mixed" phase, where both q and m order parameters are different from zero. For a sufficiently large value of J_0/J, the spin glass phase finally disappears and that region of the phase diagram is almost occupied only by the ferromagnetic phase, as shown in Fig. 5(d). For larger values of J_K/J, there remains only the Kondo phase and the transition line to the Kondo state $J_K^c(T)$ does not depend on J_0.

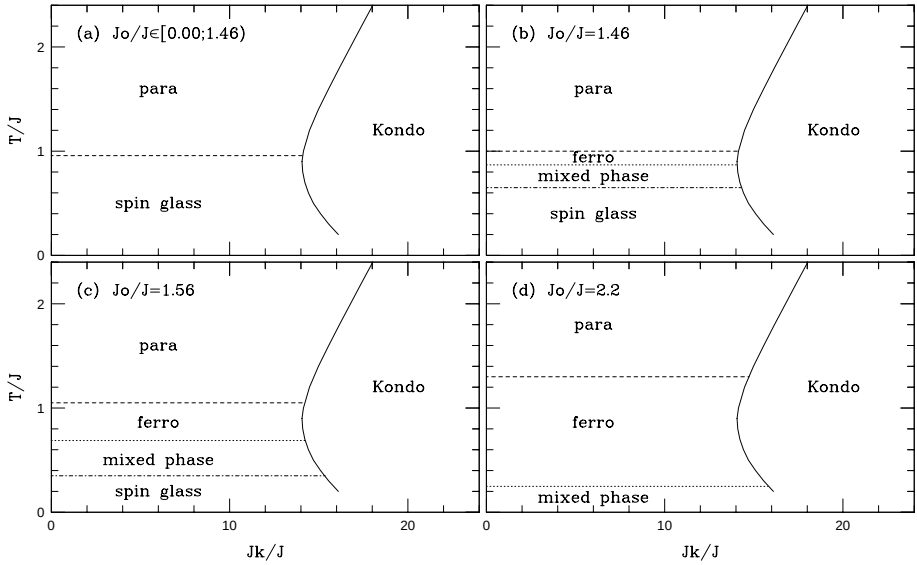

Fig. 5. Cut in the phase transition space transversal to the J_0/J axis for several values of J_0, $J = 0.5$ and $D = 10$. The solid line shows the transition from the Kondo phase to the other ones. The dashed line shows the transition from the paramagnetic phase to the ferromagnetic and the spin glass phases. One can notice that, as J_0 increases, a ferromagnetic and a mixed phase start to appear and, for some value of J_0, the spin glass phase finally disappears.

One can try to address the experimental phase diagram found in Ref. [23] for the alloys $CeNi_{1-x}Cu_x$, but theoretically if we vary only J_K with x, one obtains a ferromagnetic phase at a higher temperature than the spin glass one, in contrast to experiment. However, the equivalence between the experimental phase diagram and ours is not so straightforward since the Ni content would have to be associated to both J_0 and J_K. This could be an indication that the mechanism for the formation of magnetic phases like spin glass and ferromagnetism in $CeNi_{1-x}Cu_x$ is far more complicated than the modelling by a random inter-site interaction can address. Although recent investigations on the ferromagnetic transverse Ising spin glass suggest also the existence of a spin glass transition below the Curie temperature [55], it is plausible that this be characteristic of the Sherrington–Kirkpatrick model with a high degree of frustration. Less frustrated spin glass models [56] may sustain spin glass order above the Curie temperature and they can be more indicated for the study of the $CeNi_{1-x}Cu_x$ compounds.

To conclude on these two theoretical papers [24,25], we have firstly solved a Kondo lattice model showing the existence of a SG and a Kondo state depending on J_K/J and then we have examined a wider and more complex

region of the phase diagram including ferromagnetism. From this approach we have been able to generate a quite non-trivial phase diagram with a spin glass phase, ferromagnetism, a Kondo state and a mixed phase (spin glass and ferromagnetism). Nevertheless, the calculated spin glass freezing temperature is lower than the Curie temperature in contrast with the experimental findings [23]. The present approach might also be extended to consider an antiferromagnetic ordering, in order to explain the sequence of SG-AF-Kondo phase transitions observed in for example $Ce_2Au_{1-x}Co_xSi_3$ alloys [47].

However, the two models presented here yield an abrupt first-order transition between the spin glass state (or the ferromagnetic phase) and the Kondo state and they do not give any Quantum Critical Point at the boundary between the two regimes, in contrast with some experimental results. This point is directly connected with the fact that we have taken only a quantum Ising Hamiltonian for the spin glass term, instead of considering the full Heisenberg Hamiltonian [57]. But, in order to avoid the intricacies of the random Heisenberg model [57], we have recently developed a new theoretical calculation [58], where the Heisenberg-like coupling is replaced by a quantum Ising spin glass transverse field, which consists in both an effective random interaction among the z-components, as we have considered in [24] and an uniform transverse field in the x-direction, in order to simulate the spin-flip part; this model is the simplest way to describe the quantum mechanism of spin flipping [59].

The infinite range quantum Ising spin glass in a transverse field is the simplest model that presents a quantum critical point. It has been widely studied by using the Trotter–Suzuki technique [60], and more recently by the use of two fermionic representations of the spin operators [61] that are more suitable to our purposes.

Thus the new hamiltonian used in Ref. [58] is given by :

$$\mathcal{H} = \mathcal{H}_0 - 2G \sum_i S^x_{fi}\,, \tag{12}$$

where $\mathcal{H}_0$ is the preceding Hamiltonian given by Eq. (10).

As the transverse field G mimics the spin flip part of the Heisenberg coupling among localized spins that originates from the RKKY interaction, we use the previously proposed form [16] for G, *i.e.* $G \approx \alpha J_K^2$ where J_K is the antiferromagnetic Kondo coupling. Within this assumption, the calculation gives a phase diagram of T *versus* J_K similar to that shown in figure 4 at low temperatures, with a spin glass phase for low J_K values and a Kondo phase for high J_K values, but the transition is clearly different. The introduction of G induces a decrease, with increasing J_K, of the second-order transition

line T_{SG} that forms the spin glass boundary and tends to zero at a QCP. Also, the boundary of the Kondo state is a second-order transition line that decreases with decreasing J_K and drops to zero at a critical J_K value. The lines do not intersect, then there is not a direct transition between the spin glass and Kondo phases. A full paper [58] will be published soon on this improved model for the SG–Kondo competition.

4. Concluding remarks

Thus, we have presented here two interesting problems, the short range magnetic order-Kondo competition and the spin glass-Kondo competition, that we have both treated in a mean-field approximation. In the Kondo-lattice case, we have made a full description of the Kondo problem as a function of the intersite exchange interaction and of the conduction band filling and we have also described the short-range magnetic correlation effects which can occur in cerium compounds [20]. An important result of our model is that the Kondo temperature for the lattice could be very different from the corresponding one for the single impurity. Such an effect has been observed in a few cerium compounds such as $CeRh_2Si_2$, $CeRu_2Ge_2$ or $Ce_2Rh_3Ge_5$, but the single-impurity Kondo model seems to be in fact quite robust in other cerium compounds and in ytterbium compounds. Further experimental work is necessary to better understand the role of the different exchange interactions and of the band filling in the Kondo problem for a lattice.

On the other hand, our description of the Spin Glass-Kondo competition is able to account for some peculiar phase diagrams observed in several cerium compounds. However, we have not found the existence of a "mixed" SG-Kondo phase in cerium disordered alloys, as well as previously an antiferromagnetic-Kondo "mixed" phase [18]. This shortfall of the approximation is probably coming from the fact that mean-field schemes generally induce first-order transitions, so maybe one ought to consider the effect of fluctuations in order to get a more accurate description of the QCP. On the other hand, further experimental work is necessary, in order to better understand the interplay between spin glass, Non Fermi Liquid behavior and regular Kondo phases in cerium or uranium compounds.

REFERENCES

[1] K.G. Wilson, *Rev. Mod. Phys.* **47**, 773 (1975).

[2] P. Nozières, *J. Low Temp. Phys.* **17**, 31 (1974).

[3] K. Andres, J.E. Graebner, H.R. Ott, *Phys. Rev. Lett.* **35**, 1779 (1975).

[4] B. Coqblin, J. Arispe, A.K. Bhattacharjee, S.M.M. Evans, *Selected Topics in Magnetism, Frontiers in Solid State Sciences*, vol. 2, ed. by L.C. Gupta and M.S. Murani, World Scientific, Singapore 1993, p.75, and references therein.

[5] B. Cornut, B. Coqblin, *Phys. Rev.* **B5**, 4541 (1972).

[6] F. Steglich, J. Aarts, C.D. Bredl, W. Lieke, D. Meschede, W. Franz , *Phys. Rev. Lett.* **43**, 1892 (1979).

[7] F. Steglich, *J. Mag. Mag. Mater.* **226-230**, 1 (2001).

[8] S.S. Saxena, P. Agarwal, K. Ahilan, F.M. Grosche, R.K.W. Haselwimmer, M.J. Steiner, E. Pugh, I.R. Walker, S.R. Julian, P. Monthoux, G.G. Lonzarich, A. Huxley, I. Sheikin, D. Braithwaite, J. Flouquet, *Nature* **406**, 587 (2000).

[9] S. Doniach, *Proceedings of the "Int. Conf. on Valence Instabilities and Related Narrow-band Phenomena"*, ed. By R.D. Parks, Plenum Press, 168 (1976).

[10] B. Barbara, H. Bartholin, D. Florence, M.F. Rossignol, E. Walker, *Physica B* **86-88**, 177 (1977).

[11] T. Graf, J.D. Thompson, M.F. Hundley, R. Movshovich, Z. Fisk, D. Mandrus, R.A. Fischer, N.E. Phillips, *Phys. Rev. Lett.* **78**, 3769 (1997).

[12] K. Alami-Yadri, H. Wilhelm, D. Jaccard, *Physica B* **259-261**, 157 (1999).

[13] S. Sullow, M.C. Aronson, B.D. Rainford, P. Haen, *Phys. Rev.* Lett. **82**, 2963 (1999).

[14] H. Wilhelm, K. Alami-Yadri, B. Revaz, D. Jaccard, *Phys. Rev.* **B59**, 3651 (1999).

[15] K. Umeo, T. Takabatake, T. Suzuki, S. Hane, H. Mitamura, T. Goto, *Phys. Rev.* **B64**, 144412 (2001).

[16] J.R. Iglesias, C. Lacroix, B. Coqblin, *Phys. Rev.* **B56**, 11820 (1997).

[17] A.R. Ruppenthal, J.R. Iglesias, M.A. Gusmão, *Phys. Rev.* **B60**, 7321 (1999).

[18] B. Coqblin, M.A. Gusmão, J.R. Iglesias, C. Lacroix, A.R. Ruppenthal, Acirete S. Da R. Simoes, *Physica B* **281-282**, 50 (2000).

[19] C. Lacroix, J.R. Iglesias, B. Coqblin, *Physica B* **312-313**, 159 (2002).

[20] B. Coqblin, C. Lacroix, M.A. Gusmão, J.R. Iglesias, to appear in *Phys. Rev.* **B** (2003), `cond-mat 0212034`.

[21] B. Coqblin, M.A. Gusmão, J.R. Iglesias, A.R. Ruppenthal, C. Lacroix, *J. Magn. Magn. Mater.* **226-230**, 115 (2001).

[22] J. C. Gómez Sal, J. Garcia Soldevilla, J.A. Blanco, J.I. Espeso, J. Rodriguez Fernandez, F. Luis, F. Bartolomé, J. Bartolomé, *Phys. Rev.* **B56**, 11741 (1997).

[23] J. Garcia Soldevilla, J.C. Gomez Sal, J.A. Blanco, J.I. Espeso, J. Rodriguez Fernandez, *Phys. Rev.* **B61**, 6821 (2000).

[24] Alba Theumann, B. Coqblin, S.G. Magalhaes, A.A. Schmidt, *Phys. Rev.* **B63**, 054409 (2001).

[25] S.G. Magalhaes, A.A. Schmidt, Alba Theuman, B. Coqblin, *Eur. Phys. J.* **B30**, 419 (2002).

[26] J. Rossat-Mignod, L.P. Regnault, J.L. Jacoud, C. Vettier, P. Lejay, J. Flouquet, E. Walker, D. Jaccard, A. Amato, *J. Magn. Magn. Mater.* **76-77**, 376 (1988).

[27] J. Pierre, P. Haen, C. Vettier, S. Pujol, *Physica B* **163**, 463 (1990).

[28] J. Flouquet, S. Kambe, L.P. Regnault, P. Haen, J.P. Brison, F. Lapierre, P. Lejay, *Physica B* **215**, 77 (1995).

[29] L.P. Regnault, W.A.C. Erkelens, J. Rossat-Mignod, P. Lejay, J. Flouquet, *Phys. Rev.* **B38**, 4481 (1988).

[30] J.M. Mignot, J.L. Jacoud, L.P. Regnault, J. Rossat-Mignod, P. Haen, P. Lejay, P. Boutrouille, B. Hennion, D. Petitgrand, *Physica B* **163**, 611 (1990).

[31] L.P. Regnault, J.L. Jacoud, J.M. Mignot, J. Rossat-Mignod, C. Vettier, P. Lejay, J. Flouquet, *Physica B* **163**, 606 (1990).

[32] C. Lacroix, M. Cyrot, *Phys. Rev.* **B20**, 1969 (1979).

[33] P. Nozières, *Eur. Phys. J.* **B6**, 447 (1998).

[34] R. Jullien, P. Pfeuty, *J. Phys. F* **11**, 353 (1981).

[35] M.A. Continentino, G.M. Japiassu, A. Troper, *Phys. Rev.* **B39**, 9734 (1989).

[36] H. Tsunetsugu, Y. Hatsugai, K. Ueda, M. Sigrist, *Phys. Rev.* **B46**, 3175 (1992).

[37] S. Burdin, A. Georges, D.R. Grempel, *Phys. Rev. Lett.* **85**, 1048 (2000).

[38] S. Burdin, Ph. D. Thesis, Grenoble (2001).

[39] A.H. Castro Neto, B.A. Jones, *Phys. Rev.* **B62**, 14975 (2000).

[40] B.H. Bernhard, C. Lacroix, J.R. Iglesias, B. Coqblin, *Phys. Rev.* **B61**, 441 (2000).

[41] A.N. Tahvildar, M. Jarrell, J.K. Freericks, *Phys. Rev.* **B55**, R3332 (1997).

[42] A.J. Arko, J.J. Joyce, A.B. Andrews, J.D. Thompson, J.L. Smith, D. Mandrus, M.F. Hundley, A.L. Cornelius, E. Moshopoulou, Z. Fisk, P.C. Canfield, Alois Menovsky, *Phys. Rev.* **B56**, R7041 (1997).

[43] P. Coleman, N. Andrei, *J. Phys. C: Condens. Matter* **1**, 4057 (1989).

[44] H. Tsunetsugu, M. Sigrist, K. Ueda, *Rev. Mod. Phys.* **69**, 809 (1997).

[45] S. Schmidt, F. Reinert, D. Ehm, G. Nicolay, O. Trovarelli, C.H. Booth, R. Hauser, S. Hüfner, *Physica B* **312-313**, 675 (2002).

[46] D. Eom, M. Ishikawa, J. Kitagawa, N. Takeda, *J. Phys. Soc. Jpn.* **67**, 2495 (1998).

[47] S. Majumdar, E.V. Sampathkumaran, St. Berger, M. Della Mea, H. Michor, E. Bauer, M. Brando, J. Hemberger, A. Loidl, *Solid State Comm.* **121**, 665 (2002).

[48] E.V. Sampathkumaran, these Proceedings.

[49] M.B. Maple, M.C. de Andrade, J. Herrmann, Y. Dalichaouch, D.A. Gajewski, C.L. Seaman, R. Chau, R. Movshovich, M.C. Aronson, R. Osborn,*J. Low Temp. Phys.* **99**, 223 (1995).

[50] R. Chau, M.B. Maple, *J. Phys. C: Condens. Matter* **8**, 9939 (1996).

[51] V.S. Zapf, R.P. Dickey, E.J. Freeman, C. Sirvent, M.B. Maple, *Phys. Rev.* **B65**, 024437 (2002).

[52] D. Sherrington, S. Kirkpatrick, *Phys. Rev. Lett.* **35**, 1972 (1975).

[53] Alba Theumann, M. Vieira Gusmão, *Phys. Lett.* **A105**, 311 (1984) and Alba Theumann, *Phys. Rev.* **B33**, 559 (1986).

[54] Anirvan M. Sengupta, A. Georges, *Phys. Rev.* **B52**, 10295 (1995).

[55] Ying-Jer Kao, G.S. Grest, K. Levin, J. Brooke, T.F. Rosenbaum, G. Aeppli, *Phys. Rev.* **B64**, R060402 (2001).

[56] J.L. van Hemmen, *Phys. Rev. Lett.* **49**, 409 (1982).

[57] A. Georges, O. Parcollet, S. Sachdev, *Phys. Rev.* **B63**, 134406 (2001).

[58] Alba Theumann, B. Coqblin, to be published.

[59] M.J. Rozenberg, L. Arrachea, *Physica B* **312-313**, 416 (2002).

[60] Yadin Goldschmidt, Pik-Lin Lai, *Phys. Rev. Lett.* **64**, 2467 (1990).

[61] Alba Theumann, A.A. Schmidt, S.G. Magalhaes, *Physica A* **311**, 498 (2002).